MIML Workshop, May 13th 2022
CMIC, University College London
London, UK

Data-driven, model-free, deep learning approach for quantitative MRI protocol design

Francesco Grussu[1,2]

[1]Honorary Senior Fellow, Queen Square MS Centre, QS Institute of Neurology, Faculty of Brain Sciences, University College London (UCL), London, UK

[2]Beatriu de Pinós Fellow, Radiomics Group, Vall d'Hebron Institute of Oncology, Vall d'Hebron Barcelona Hospital Campus, Barcelona, Spain

Contact:

f.grussu@ucl.ac.uk fgrussu@vhio.net

Outline of the talk

- Introduction
  - *quantitative MRI (qMRI)*
  - *qMRI protocol optimisation*

Outline of the talk

- Introduction
  - *quantitative MRI (qMRI)*
  - *qMRI protocol optimisation*

- Select and Retrieve via Direct Upsampling network (SARDU-Net)
  - *protocol selection: brain and prostate diffusion-relaxation imaging*
  - *signal prediction: MUDI challenge*
  - *methodological considerations*

Outline of the talk

- Introduction
  - *quantitative MRI (qMRI)*
  - *qMRI protocol optimisation*

- Select and Retrieve via Direct Upsampling network (SARDU-Net)
  - *protocol selection: brain and prostate diffusion-relaxation imaging*
  - *signal prediction: MUDI challenge*
  - *methodological considerations*

- Progressive Subsampling for Oversampled Data (PROSUB)

Outline of the talk

- Introduction
  - *quantitative MRI (qMRI)*
  - *qMRI protocol optimisation*

- Select and Retrieve via Direct Upsampling network (SARDU-Net)
  - *protocol selection: brain and prostate diffusion-relaxation imaging*
  - *signal prediction: MUDI challenge*
  - *methodological considerations*

- Progressive Subsampling for Oversampled Data (PROSUB)

- Discussion and conclusions

Introduction: qMRI

- In quantitative MRI (qMRI), sets of multi-contrast images are analysed to estimate biophysical properties of tissues in each image voxel

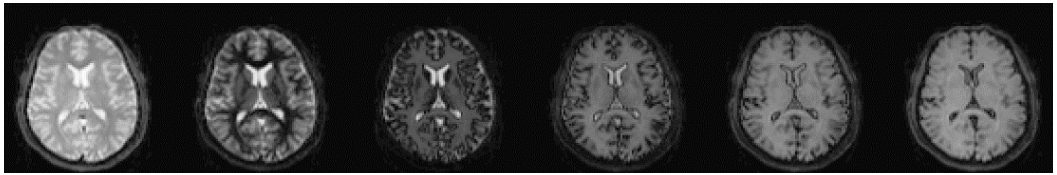

$$s = s_0 \left| 1 - 2\, e^{-\frac{TI}{T1}} \right|$$

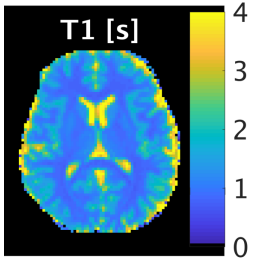

Introduction: qMRI

- In quantitative MRI (qMRI), sets of multi-contrast images are analysed to estimate biophysical properties of tissues in each image voxel

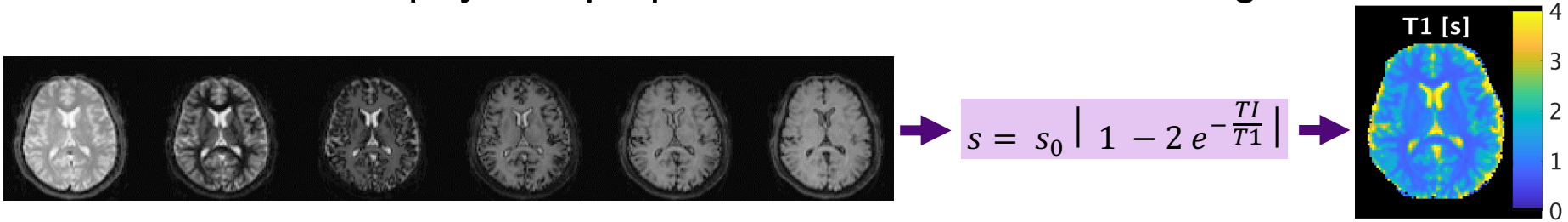

- **qMRI protocol:** set of sequence parameter settings to use to produce such a multi-contrast MRI acquisition

→ e.g., TI = {80ms, 160ms, 320ms, 640ms, 1280ms, 2560ms}

Model-based protocol optimisation

- **Optimisation** → find a protocol that is *optimum* according to some criterion

Model-based protocol optimisation

- **Optimisation** → find a protocol that is *optimum* according to some criterion
- **Model-based approach** → *optimality* is based on an explicit signal model [1]

[1] Alexander D, Magnetic Resonance in Medicine 2008, doi: doi:10.1002/mrm.21646

Model-based protocol optimisation

- **Optimisation** → find a protocol that is *optimum* according to some criterion
- **Model-based approach** → *optimality* is based on an explicit signal model [1]

1. Define the signal model, e.g., $s = \sum_n^N f_n \, e^{-b \, D_n}$
2. Define the expected distribution of tissue parameters $\mathbf{p} = (f_1, D_1, f_2, D_2, \dots)$
3. Define the noise level σ
4. Define an optimality criterion, e.g., minimum Cramer-Rao Bound $J^{-1}(b; \mathbf{p}, \sigma)$
5. Find M sequence parameter configurations that maximise optimality:

$$(b_1, b_2, \dots, b_M) = \arg\min \sum_{\mathbf{p}} J^{-1}(b; \mathbf{p}, \sigma)$$

[1] Alexander D, Magnetic Resonance in Medicine 2008, doi: doi:10.1002/mrm.21646

Data-driven protocol optimisation

- **Model-based protocol optimisation comes with assumptions**
  - *the signal model itself*
  - *the range of variation of tissue parameters*
  - *the noise level*

Data-driven protocol optimisation

- **Model-based protocol optimisation comes with assumptions**
  - *the signal model itself*
  - *the range of variation of tissue parameters*
  - *the noise level*

- **Data-driven optimisation** → learn compact protocols from rich pilot scans
  - *no assumptions on signal models, tissue parameters, noise levels*
  - *test scans are commonly performed when setting up new studies*
  - *useful when the model of interest is not known/fixed*

The SARDU-Net framework

Select And Retrieve via Direct Upsampling Network (SARDU-Net)

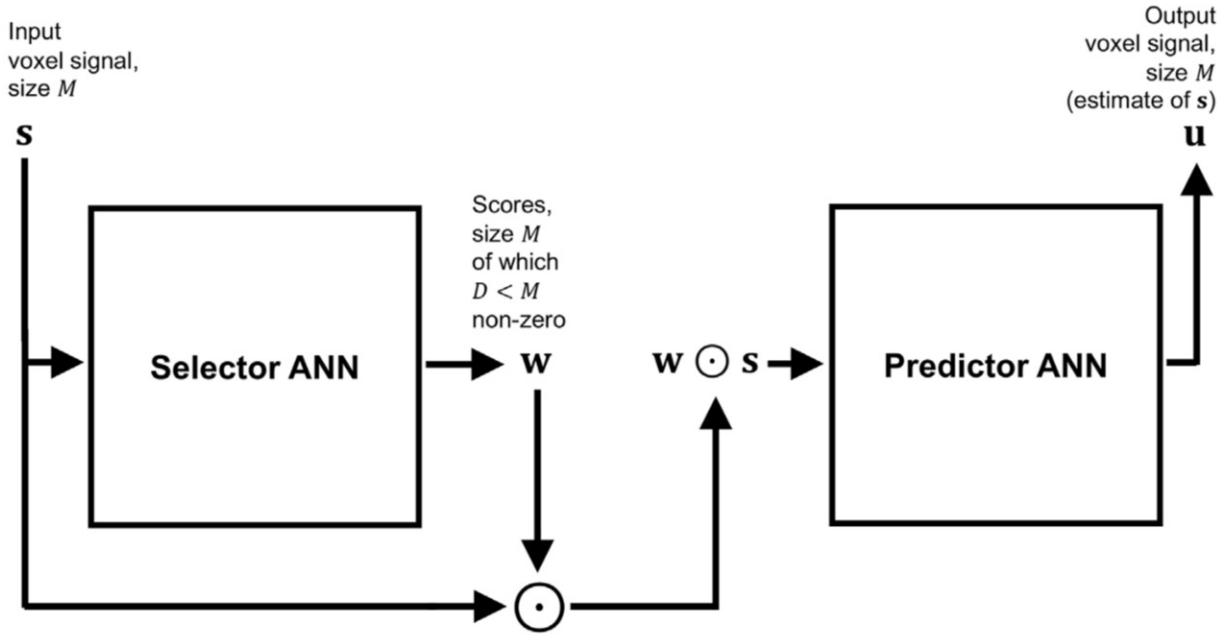

1) Perform a few rich qMRI acquisitions of M measurements

2) Find a maximally informative subset of $D < M$ measurements

3) Use the qMRI protocol of size D for your prospective study

[2] Grussu F et al, Frontiers in Physics 2021, doi: 10.3389/fphy.2021.752208

https://github.com/fragrussu/sardunet

Selector and Predictor networks

Achitecture

- Multi-layer, fully-connected feedforward networks implemented in PyTorch

Network training

- Loss based on the signal reconstruction error
  → $L = \| s - u(s \odot w) \|_2^2$
- ADAM optimiser [3] with dropout regularisation

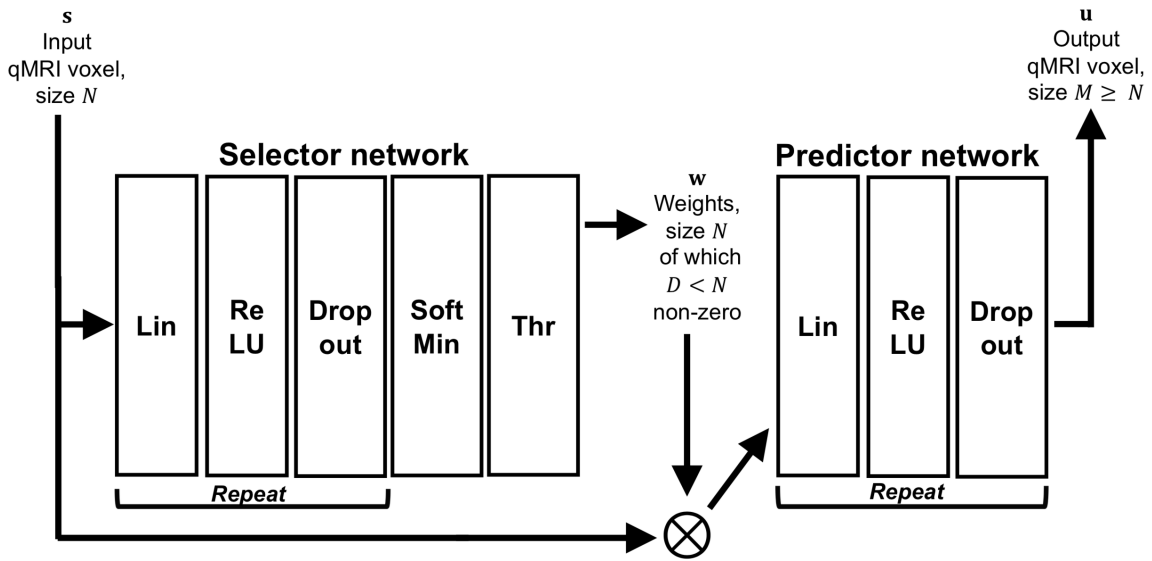

[3] Kingma DP and Ba J. Proc 3rd Int Conf Learn Represent (2015), http://arxiv.org/abs/1412.6980

SARDU-Net demonstration: brain MRI (1)

3 healthy subjects scanned on a 3T Philips Ingenia CX

- saturation inversion recovery (SIR) [4] diffusion-weighted (DW) spin echo EPI
- 528 images with 32 unique (*b*,TI)
  - b = {0, 1000, 2000, 3000} s/mm^2
  - TI = {70, 320, 570, 820, 1070, 1320, 1570, 1820} ms
  - 21 directions per (*b*,TI)
- TS = 300 ms (saturation time)
- TE = 90 ms
- TR = 2563 ms
- 2.4 mm isotropic resolution
- SENSE = 2
- Multiband factor = 3
- Scan time = 45 min

[4] Wang H et al, J Magn Reson 2017, doi:10.1016/ j.jmr.2016.11.015

SARDU-Net demonstration: brain MRI (2)

- **Find subsets** of $D = \{4, 8, 16\}$ out of $M = 32$ measurements
- **Fit a model** of diffusion-T1 relaxation [5,6] …

$$s(b,\ \mathrm{TI},\ \mathrm{TS}) = \frac{\sqrt{\pi}}{2} s_0 \left| 1 - e^{-\frac{\mathrm{TI}}{T_1}} - \left(1 - e^{-\frac{\mathrm{TS}}{T_1}}\right) e^{-\frac{\mathrm{TI}}{T_1}} \right| e^{-bd_\perp} \frac{\mathrm{erf}\left(\sqrt{b(d_\parallel - d_\perp)}\right)}{\sqrt{b(d_\parallel - d_\perp)}}$$

- … and **predict fully-sampled signals** based on the fitted parameters
- **Assess the quality of reconstructed signals/metrics** against:
  - *random sub-protocols*
  - *uniform down-sampling*
  - *geometric down-sampling*

[5] De Santis S et al, NeuroImage 2016, doi:10.1016/j.neuroimage.2016.07.037
[6] Kaden E et al, Magn Reson Med 2016, doi:10.1002/mrm.25734

Results: brain sub-protocol selection

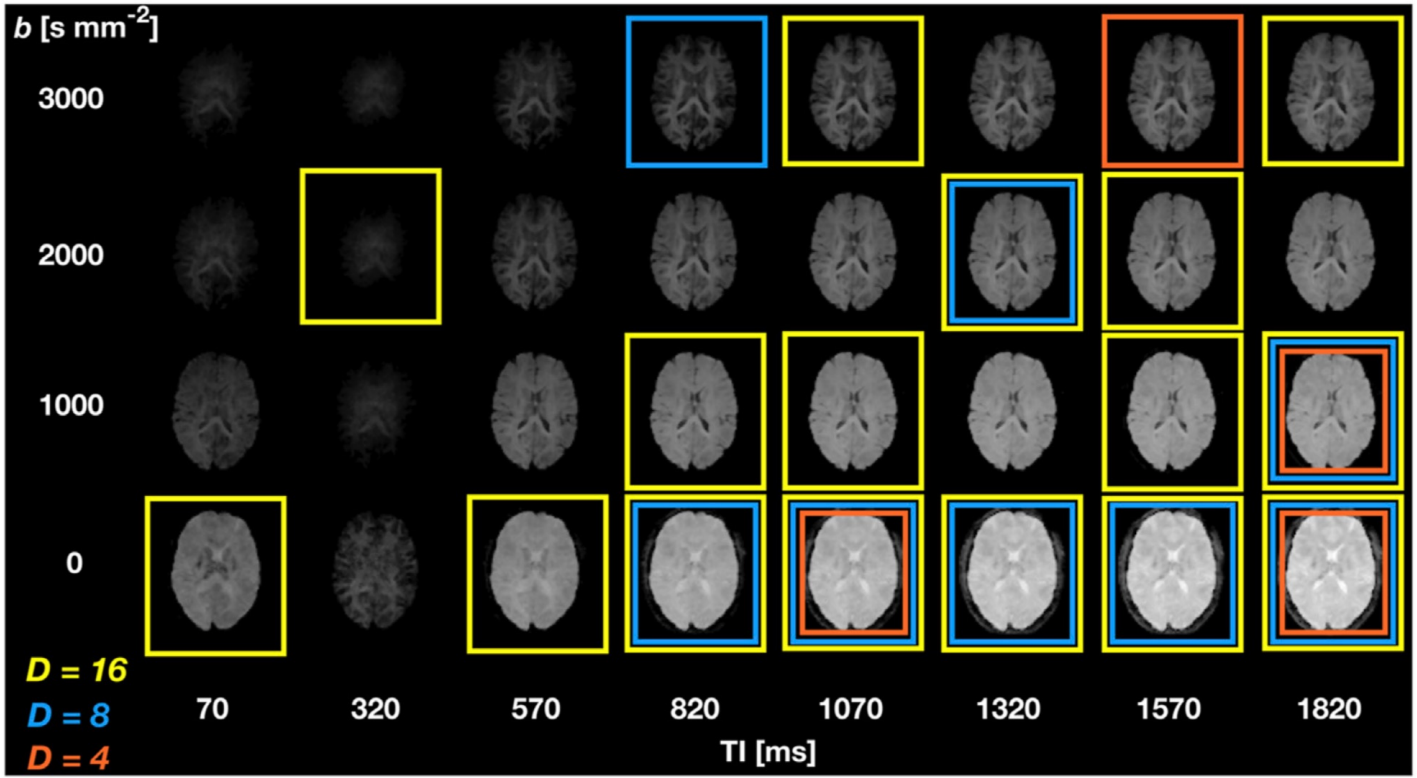

- A variety of contrasts are sampled
- SNR plays a role, but high *b*-values are always selected

Results: selection reproducibility

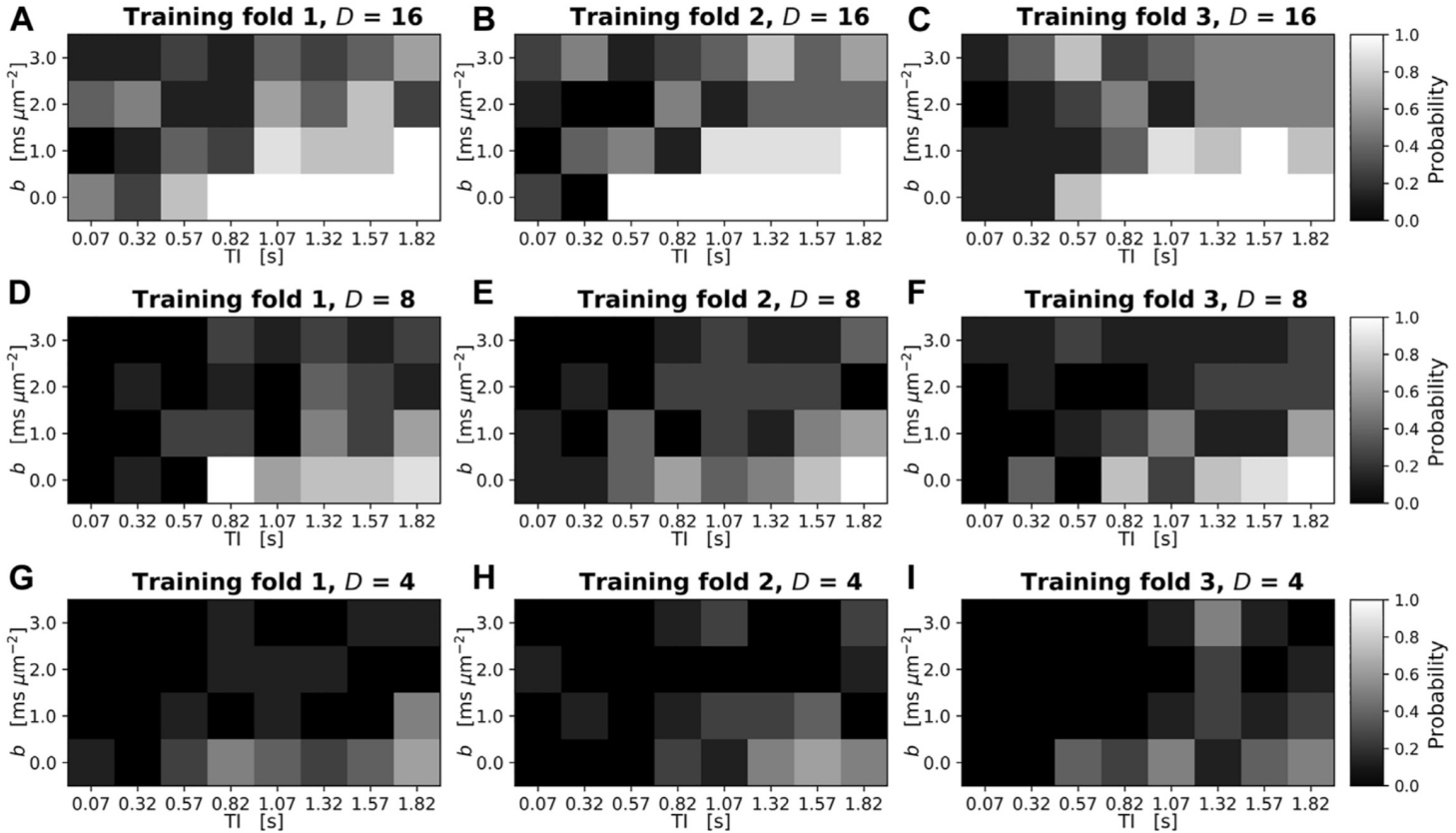

- Sub-protocol selection consistent across training folds and initialisations
- Some variability is seen

Results: parametric maps

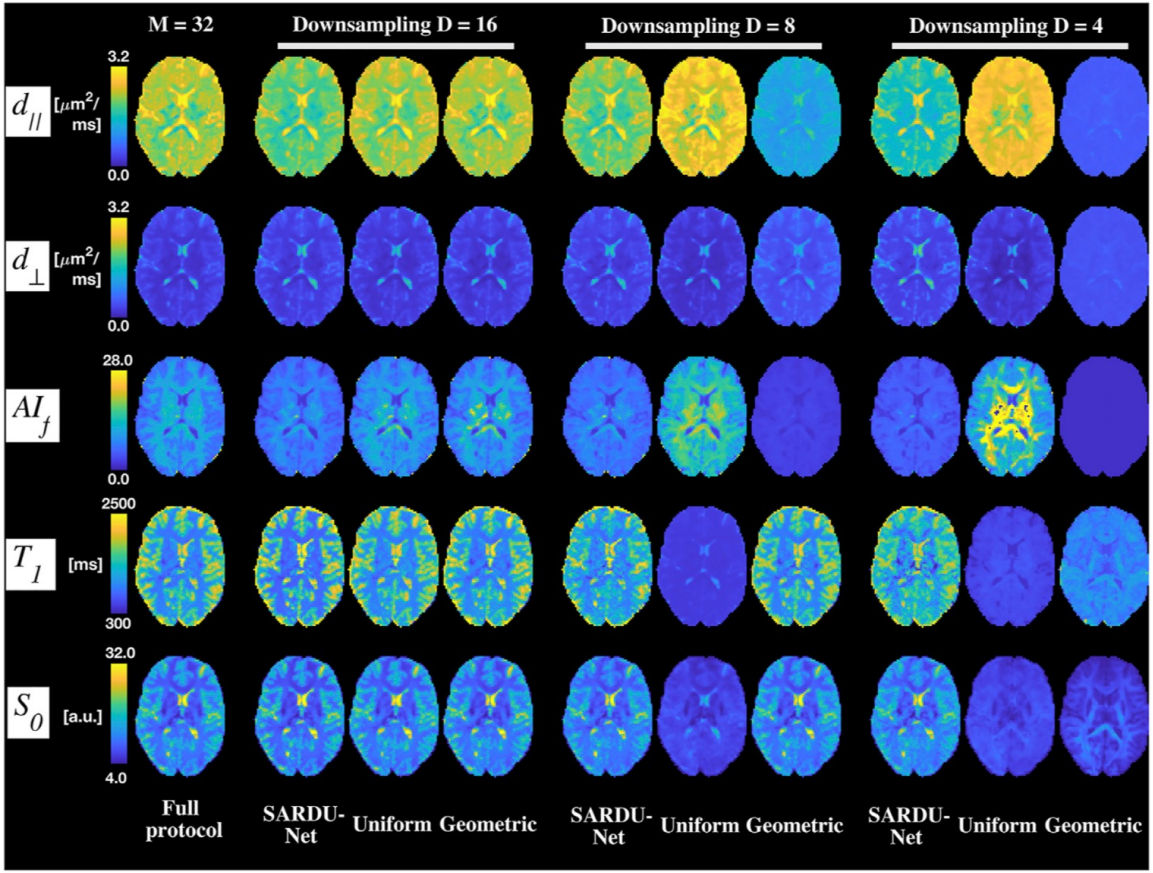

- For low sub-sampling rates, uniform and geometric sub-protocols work just fine
- For aggressive sub-sampling, SARDU-Net sub-protocols enable better map computation

Results: differences w. r. t. reference

TABLE 1 | Results of the SARDU-Net, uniform and geometric sub-protocol comparison against a null distribution from randomly selected sub-protocols (brain data, T1-SMDT model).

		Signal MSE [a.u.]			$d_{\parallel}$ difference [$\mu m^2\ ms^{-1}$]			$d_{\perp}$ difference [$\mu m^2\ ms^{-1}$]			T_1 difference [ms]			s_0 difference [a.u.]		
D/*M*	Sub-sampling	Subj. 1	Subj. 2	Subj. 3	Subj. 1	Subj. 2	Subj. 3	Subj. 1	Subj. 2	Subj. 3	Subj. 1	Subj. 2	Subj. 3	Subj. 1	Subj. 2	Subj. 3
16/32	SARDU-Net	**0.162 (q=0.003)***	**0.104 (q=0.09)**	**0.195 (q=0.001)***	− 0.048 (q=0.63)	**− 0.018 (q=0.12)**	0.026 (q=0.23)	0.026 (q=0.91)	0.028 (q=0.82)	0.017 (q=0.72)	13.2 (q=0.33)	9.2 (q=0.20)	21.1 (q=0.25)	0.384 (q=0.33)	0.238 (q=0.25)	0.540 (q=0.20)
	Uniform	0.170 (q=0.24)	0.165 (q=0.23)	0.204 (q=0.19)	**0.005 (q=0.06)**	0.019 (q=0.13)	**− 0.023 (q=0.21)**	− 0.008, (q=0.47)	− 0.012 (q=0.56)	− 0.010 (q=0.48)	**6.0 (q=0.17)**	**− 7.6 (q=0.17)**	**−3.7 (q=0.03)***	**0.221 (q=0.19)**	**− 0.157 (q=0.19)**	− 0.453 (q=0.14)
	Geometric	0.177 (q=0.43)	0.107 (q=0.36)	0.224 (q=0.58)	0.028 (q=0.44)	0.019 (q=0.13)	0.051 (q=0.39)	**0.002 (q=0.12)**	**− 0.003 (q=0.17)**	**0.007 (q=0.39)**	− 19.1 (q=0.46)	18.0 (q=0.39)	− 7.9 (q=0.08)	0.410 (q=0.36)	0.229 (q=0.24)	**0.082 (q=0.02)***
	95% range	[0.165; 0.482]	[0.103; 0.565]	[0.199; 0.584]	[−0.121: 0.086]	[−0.207; 0.146]	[−0.258; 0.178]	[−0.040; 0.020]	[−0.093; 0.022]	[−0.061; 0.024]	[−177.4; 63.1]	[−214.7; 88.4]	[−274.0; 71.9]	[−7.088; 1.439]	[−9.902; 1.212]	[-9.54; 1.29]
8/32	SARDU-Net	**0.182 (q=0.05)***	**0.116 (q=0.12)**	**0.214 (q=0.04)***	− 0.033 (q=0.26)	0.127 (q=0.53)	**0.021 (q=0.09)**	0.045 (q=0.82)	**0.002 (q=0.04)***	**0.032 (q=0.57)**	37.8 (q=0.40)	**20.8 (q=0.23)**	53.0 (q=0.36)	0.970 (q=0.37)	**0.083 (q=0.04)***	0.992 (q=0.28)
	Uniform	0.545 (q=0.84)	0.503 (q=0.61)	0.558 (q=0.78)	**0.018 (q=0.13)**	**0.027 (q=0.10)**	− 0.039 (q=0.16)	**− 0.027 (q=0.61)**	− 0.038 (q=0.55)	− 0.037 (q=0.60)	455.8 (q=0.99)	547.9 (q=0.99)	351.9 (q=0.99)	18.01 (q=0.99)	18.27 (q=0.99)	12.20 (q=0.97)
	Geometric	0.235 (q=0.28)	0.189 (q=0.52)	0.294 (q=0.32)	− 0.471 (q=0.98)	−0.486 (q=0.97)	− 0.500 (q=0.97)	0.064 (q=0.91)	0.014 (q=0.27)	0.054 (q=0.74)	**8.2 (q=0.14)**	43.5 (q=0.40)	**26.0 (q=0.17)**	**0.463 (q=0.18)**	0.929 (q=0.41)	**0.985 (q=0.28)**
	95% range	[0.177; 1.483]	[0.107; 2.140]	[0.215; 1.984]	[−0.350; 0.344]	[−0.425; 0.384]	[−0.498; 0.391]	[−0.084; 0.053]	[−0.147; 0.042]	[−0.111; 0.053]	[−281.7; 109.0]	[−265.5; 146.5]	[−339.5; 92.2]	[−11.76; 2.825]	[−12.32; 2.913]	[−12.26; 2.107]
4/32	SARDU-Net	**0.202 (q=0.002)***	**0.122 (q=0.01)***	**0.235 (q=0.001)***	**0.016 (q=0.05)***	−0.210 (q=0.35)	0.093 (q=0.16)	0.035 (q=0.41)	0.045 (q=0.28)	0.046 (q=0.38)	**53.6 (q=0.24)**	**81.8 (q=0.29)**	**99.5 (q=0.30)**	**1.56 (q=0.20)**	**1.46 (q=0.15)**	2.46 (q=0.24)
	Uniform	0.659 (q=0.55)	0.603 (q=0.52)	0.649 (q=0.50)	− 0.181 (q=0.39)	− 0.211 (q=0.35)	− 0.218 (q=0.36)	**−0.002 (q=0.03)***	**− 0.017 (q=0.12)**	**− 0.015 (q=0.13)**	196.7 (q=0.62)	260.7 (q=0.78)	107.8 (q=0.32)	4.27 (q=0.44)	3.04 (q=0.24)	**0.07 (q=0.006)***
	Geometric	1.250 (q=0.66)	1.231 (q=0.66)	1.353 (q=0.66)	− 0.020 (q=0.07)	**− 0.033 (q=0.06)**	**0.039 (q=0.06)**	−0.031 (q=0.37)	− 0.122 (q=0.69)	− 0.068 (q=0.58)	− 59.7 (q=0.27)	−159.7 (q=0.53)	−213.0 (q=0.56)	− 2.18 (q=0.28)	−9.92 (q=0.67)	7.67 (q=0.58)
	95% range	[0.257; 2.544]	[0.138; 2.547]	[0.309; 0.294]	[−1.00; 0.543]	[−1.08; 0.550]	[−1.11; 0.596]	[−0.158; 0.174]	[−0.218; 0.153]	[−0.190; 0.180]	[−531.4; 277.9]	[−501.8; 294.5]	[−643.3; 250.4]	[−15.58; 8.85]	[−14.48; 7.02]	[−14.48; 5.24]

For each sub-protocol and sub-sampling factor, the table reports subject-wise signal MSE and mean differences of parametric maps with respect to maps obtained from fully sampled signals via dictionary fitting. The table also reports the 95% inclusion ranges of the random sub-protocol distribution, and the closest quantile from the random sub-protocol distribution to which MSEs and parametric map differences (in absolute value) correspond. The lowest MSE/parametric map differences among SARDU-Net, uniform and geometric sub-sampling is shown in bold font. Asterisks flag cases where the quantile q is $q \leq 0.05$.

- SARDU-Net sub-protocols enable the best signal reconstruction using a model they were not optimised for
- However, this does not imply that parametric maps are the closest to the reference

SARDU-Net demonstration: prostate MRI (1)

3 healthy subjects scanned on a 3T Philips Achieva

- DW spin echo EPI with variable TE
- 48 images with 16 unique (*b*,TE)
  - b = {0, 500, 1000, 1500} s/mm^2
  - TE = {55, 87, 121, 150} ms
  - 3 directions per (*b*,TE)
- TR = 2800 ms
- resolution: 1.75 mm × 1.75 mm × 5 mm
- SENSE = 1.6, partial Fourier factor = 0.62
- Scan time = 6 min

SARDU-Net demonstration: prostate MRI (2)

- **Find subsets** of $D = \{9, 12\}$ out of $M = 16$ measurements
- **Fit a model** of diffusion-T2 relaxation [7] …

$$s(b, \mathrm{TE}) = s_0 \left(v_l \, e^{-b\, d_l - \frac{\mathrm{TE}}{T_{2l}}} + (1 - v_l) \left(v_e \, e^{-b\, d_e - \frac{\mathrm{TE}}{T_{2e}}} + (1 - v_e)\, e^{-b\, d_s - \frac{\mathrm{TE}}{T_{2s}}} \right) \right)$$

- … and **predict fully-sampled signals** based on the fitted parameters
- **Assess the quality of reconstructed signals/metrics** against:
  - *random sub-protocols*
  - *uniform down-sampling*
  - *geometric down-sampling*

[7] Chatterjee A et al, Radiology (2018) 287:864–73. doi:10.1148/radiol.2018171130

Results: prostate sub-protocol selection

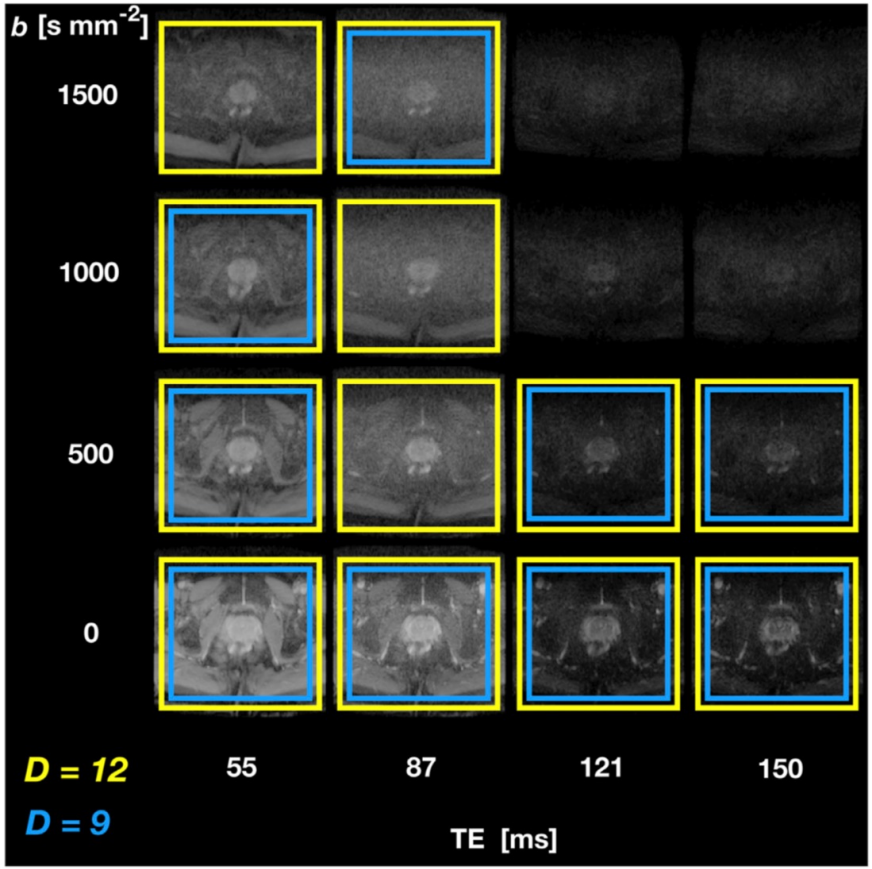

- A variety of contrasts are sampled
- SNR plays a role on measurement selection
- However, for strong sub-samplings, images with lower SNR may be preferred to images with higher SNR

Results: selection reproducibility

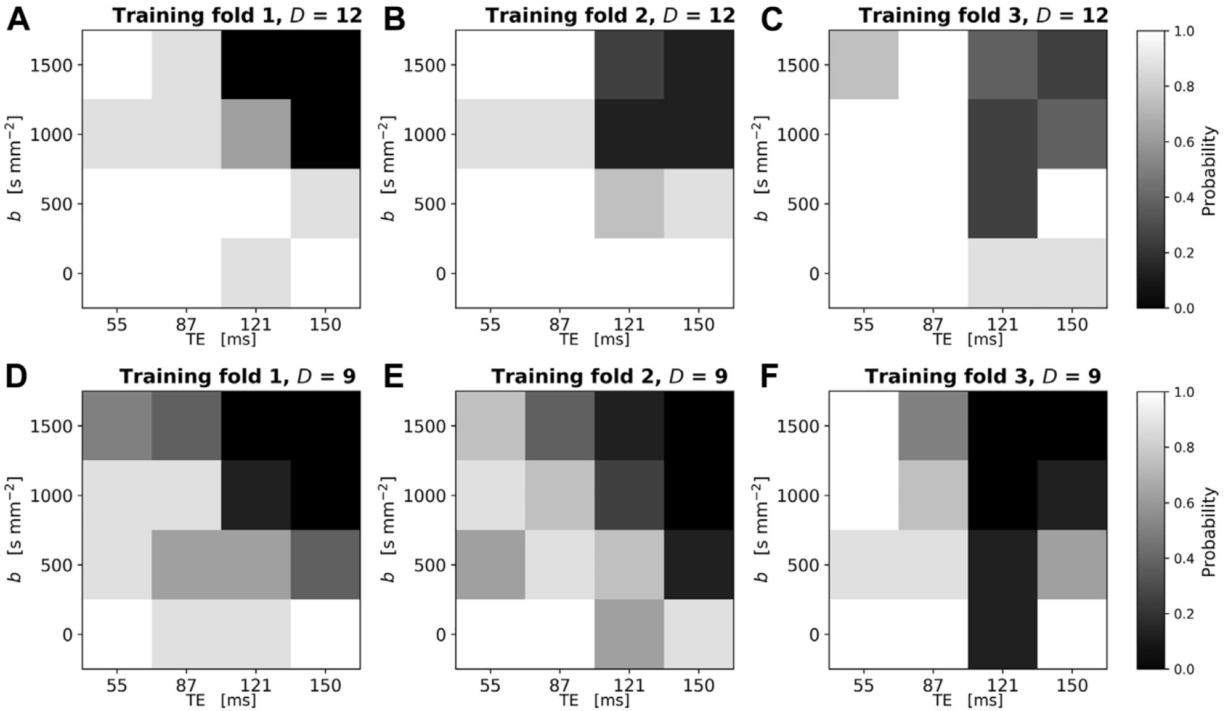

- Sub-protocol selection consistent across training folds and initialisations
- Some variability is seen

Results: parametric maps

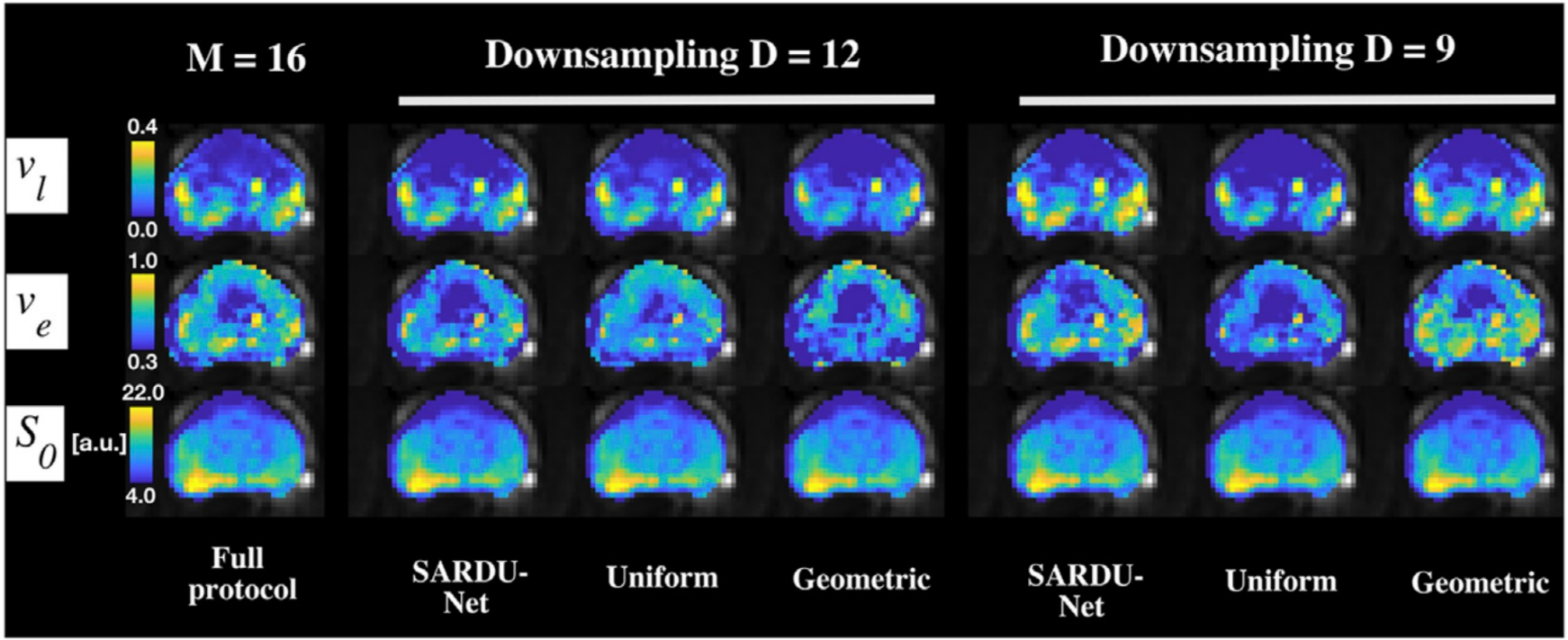

- Parametric maps from SARDU-Net sub-protocols have similar quality to the reference maps on visual inspection

Results: differences w. r. t. reference

TABLE 2 | Results of the SARDU-Net, uniform and geometric sub-protocol comparison against a null distribution obtained from all possible sub-protocols (prostate data, HM-MRI model). The bold font indicates the lowest MSE/lowest parametric map difference among values obtained for SARDU-Net, uniform and geometric sub-samplings.

D/M	Sub-sampling	Signal MSE [a.u.]			v_l difference			v difference			s_0 difference [a.u.]		
		Subj. 1	Subj. 2	Subj. 3	Subj. 1	Subj. 2	Subj. 3	Subj. 1	Subj. 2	Subj. 3	Subj. 1	Subj. 2	Subj. 3
12/16	SARDU-Net	**0.80 (q= 0.01)***	**0.43 (q = 0.01)***	**0.047 (q = 0.02)***	–0.0006 (q = 0.001)*	**– 0.001 (q = 0.02)***	– 0.006 (q = 0.23)	**0.01 (q = 0.04)***	**0.001 (q = 0.006)***	**– 0.028 (q = 0.32)**	**0.02 (q = 0.21)**	**0.006 (q = 0.07)**	**– 0.001 (q = 0.07)**
	Uniform	1.13 (q = 0.88)	0.51 (q = 0.69)	0.051 (q = 0.31)	0.01 (q = 0.001)*	– 0.04 (q = 0.41)	– 0.012 (q = 0.40)	0.23 (q = 0.77)	– 0.21 (q = 0.65)	– 0.052 (q = 0.49)	– 0.08 (q = 0.70)	0.079 (q = 0.64)	0.015 (q = 0.51)
	Geometric	0.90 (q = 0.16)	0.44 (q = 0.14)	0.050 (q = 0.25)	**0.0005 (q = 0.001)***	– 0.002 (q = 0.03)*	**0.003 (q = 0.12)**	0.06 (q = 0.06)	0.08 (q = 0.29)	0.062 (q = 0.55)	0.08 (q = 0.67)	0.076 (q = 0.63)	0.034 (q = 0.76)
	95% range	[0.88; 2.03]	[0.44; 0.76]	[0.048; 0.080]	[0.001; 0.39]	[– 0.07; 0.16]	[– 0.05; 0.06]	[– 0.22; 0.60]	[– 0.26; 0.37]	[– 0.127; 0.220]	[– 0.12; 0.24]	[– 0.30; 0.13]	[– 0.067; 0.049]
9/16	SARDU-Net	**0.88 (q = 0.01)***	**0.46 (q = 0.06)**	**0.052 (q = 0.06)**	**–0.00004 (q = 0.001)***	0.088 (q = 0.69)	**0.025 (q = 0.41)**	**0.006 (q = 0.01)***	0.23 (q = 0.51)	**0.031 (q = 0.17)**	**– 0.01 (q = 0.06)**	**0.04 (q = 0.17)**	**– 0.002 (q = 0.03)***
	Uniform	1.05 (q = 0.51)	0.58 (q = 0.56)	0.058 (q = 0.25)	–0.0006 (q = 0.001)*	– 0.059 (q = 0.34)	– 0.026 (q = 0.42)	0.214 (q = 0.49)	– 0.25 (q = 0.54)	– 0.087 (q = 0.42)	– 0.03 (q = 0.20)	0.12 (q = 0.55)	0.033 (q = 0.56)
	Geometric	0.97 (q = 0.35)	0.47 (q = 0.09)	0.053 (q = 0.09)	0.02 (q = 0.64)	**0.048 (q = 0.28)**	0.020 (q = 0.35)	– 0.181 (q = 0.42)	**0.09 (q = 0.21)**	0.044 (q = 0.23)	– 0.02 (q = 0.11)	0.05 (q = 0.18)	0.022 (q = 0.39)
	95% range	[0.89; 2.56]	[0.45; 1.27]	[0.050; 0.168]	[0.001; 0.44]	[– 0.073; 0.345]	[– 0.060; 0.167]	[– 0.251; 0.615]	[– 0.31; 0.37]	[– 0.157; 0.314]	[– 0.24; 0.60]	[– 0.40; 0.28]	[– 0.076; 0.117]

For each sub-protocol and sub-sampling factor, the table reports subject-wise signal MSE and mean differences of parametric maps with respect to maps obtained from fully sampled signals via dictionary fitting. The table also reports the 95% inclusion ranges of all sub-protocol distribution, and the closest quantile from the all sub-protocol distribution to which MSEs and parametric map differences (in absolute value) correspond. The lowest MSE/parametric map differences among SARDU-Net, uniform and geometric sub-sampling is shown in bold font. Asterisks flag cases where the quantile q is $q \leq 0.05$.

- SARDU-Net sub-protocols enable the best signal reconstruction using a model they were not optimised for
- However, this does not imply that parametric maps are the closest to the reference

qMRI upsampling

- The Predictor module effectively learns how to up-sample in qMRI space

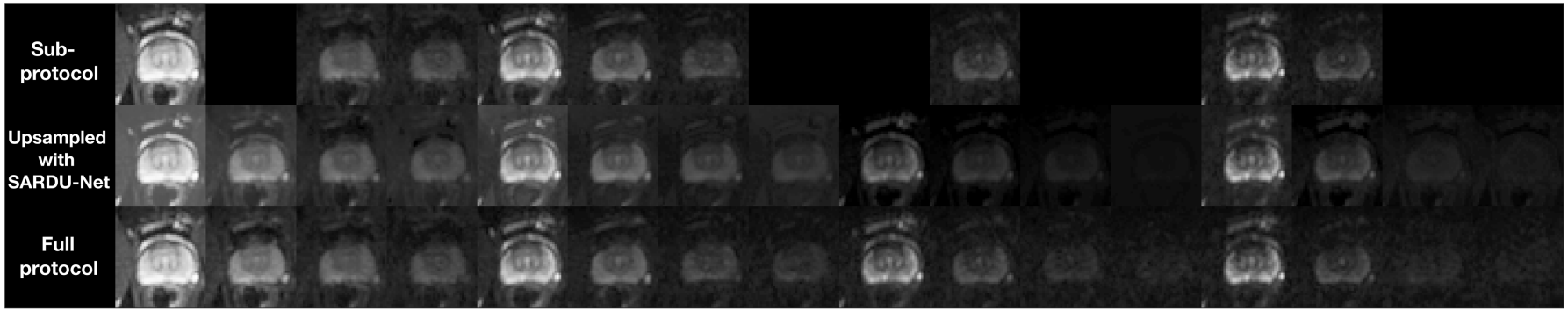

qMRI upsampling

- The Predictor module effectively learns how to up-sample in qMRI space

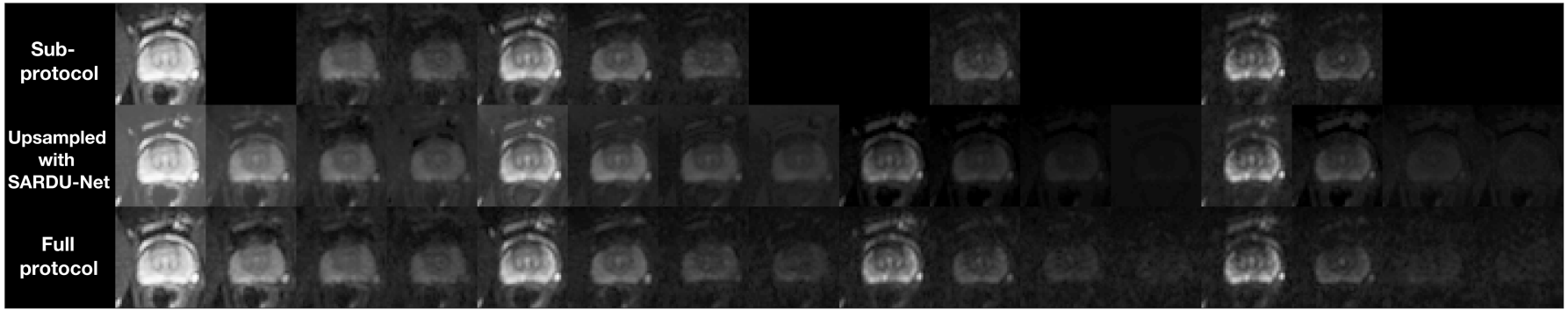

- SARDU-Net was used in the **2019 MICCAI MUDI Challenge** [8]
  - 1344 EPI volumes with variable (*b*,**g**,TI,TE) provided for 5 subjects
  - participants ask for subsets of 50, 100, 250, 500 measurements in 3 subjects
  - participants predict the full set of 1344 measurements in those 3 subjects

[8] Pizzolato M et al, Proc of Computational Diffusion MRI 2019, doi: 10.1007/978-3-030-52893-5_17

qMRI upsampling: MUDI (1)

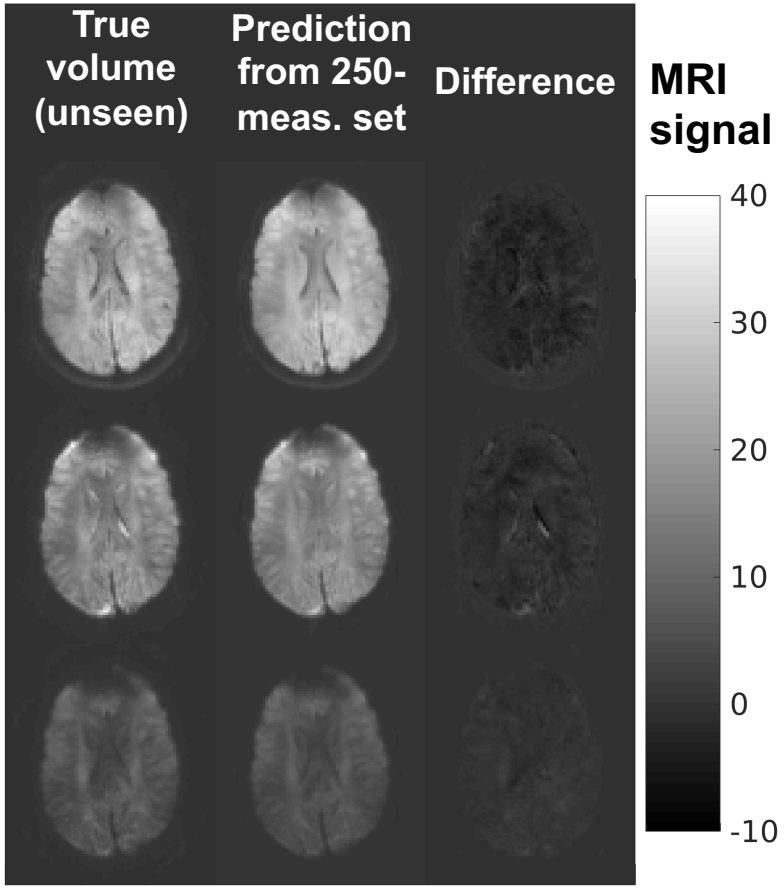

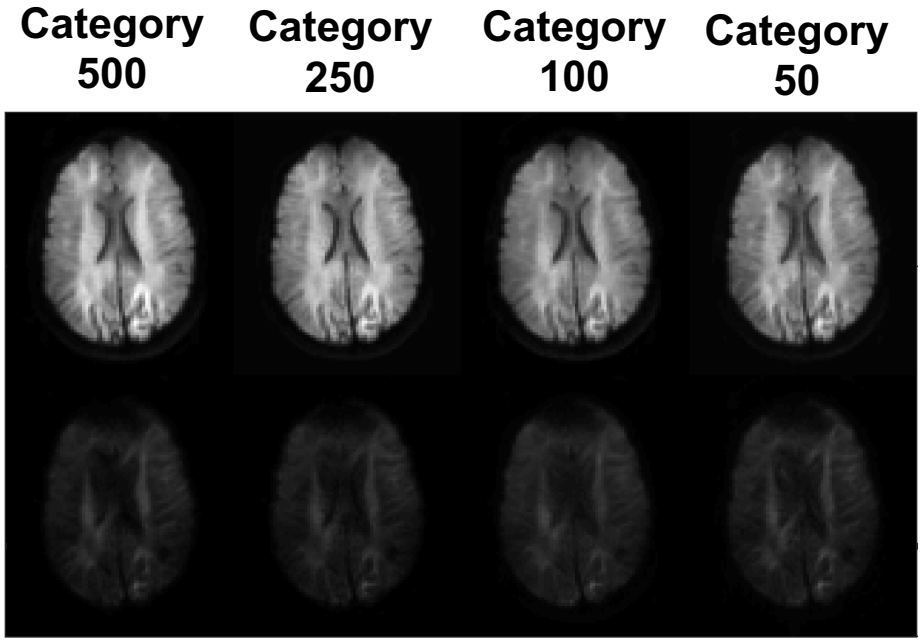

qMRI upsampling: MUDI (2)

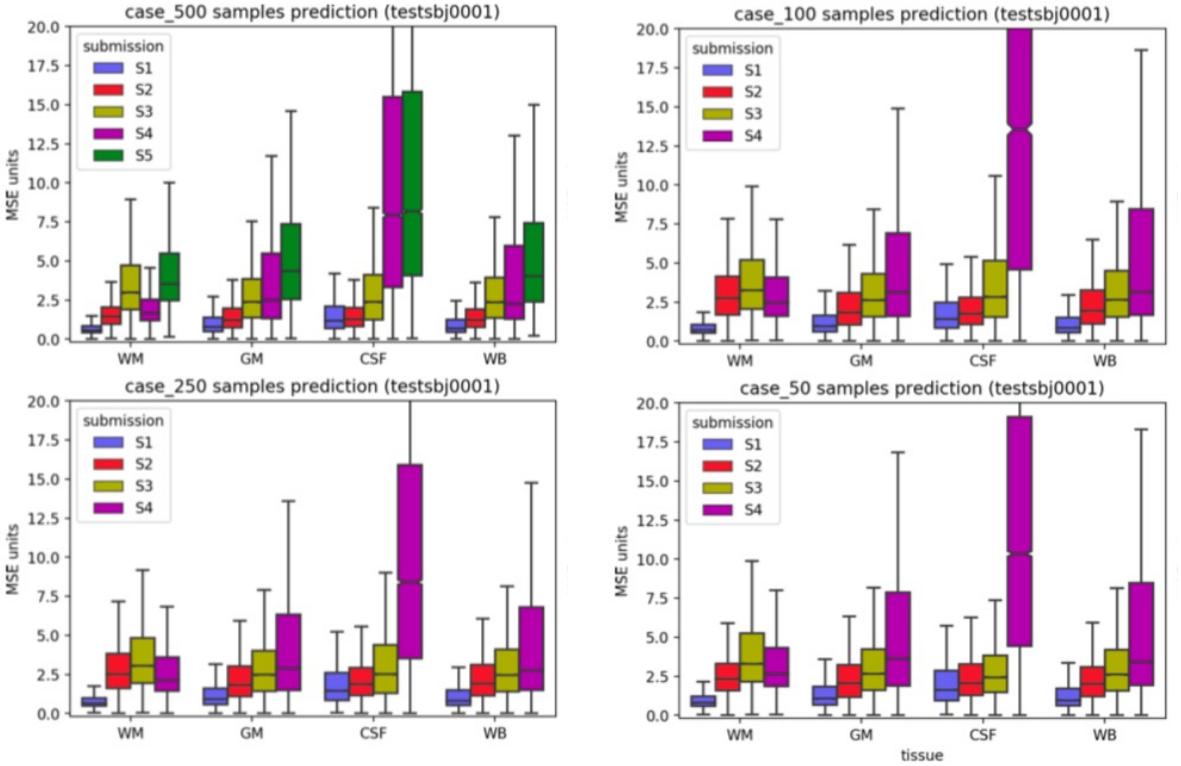

- Ranked 1st on the Challenge Day at MICCAI 2019
- Ranked 2nd when the Challenge was reopened until Spring 2020

Methodological consideration

- SARDU-Net is promising but …
  - ➢ *training stability could be improved*
  - ➢ *which architecture is best?*
  - ➢ *can we avoid **hard** thresholding?*

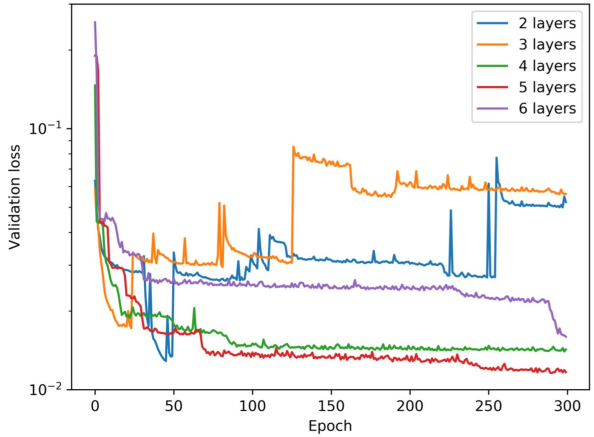

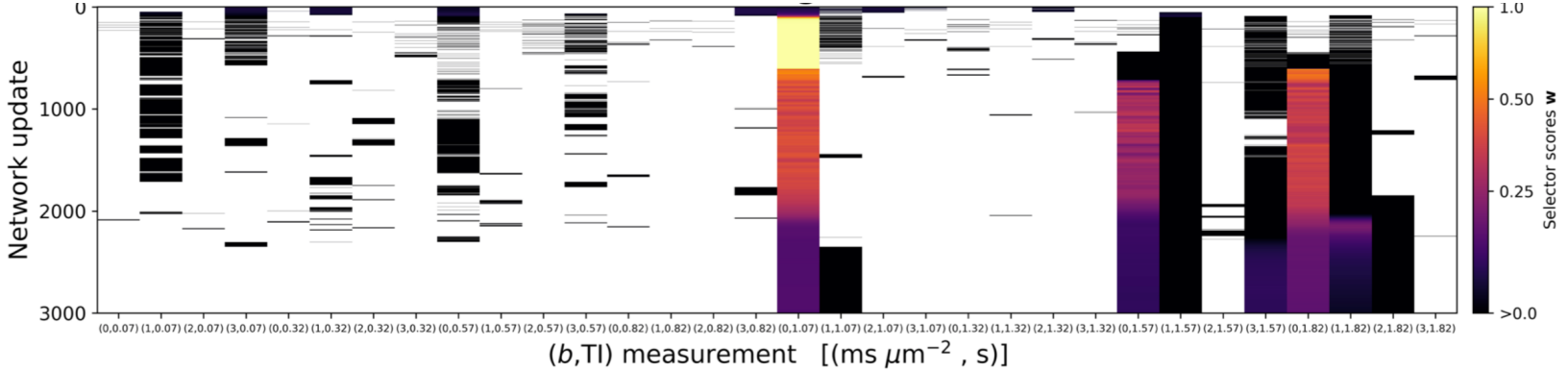

The PROSUB framework

Progressive Subsampling for Oversampled Data (PROSUB)

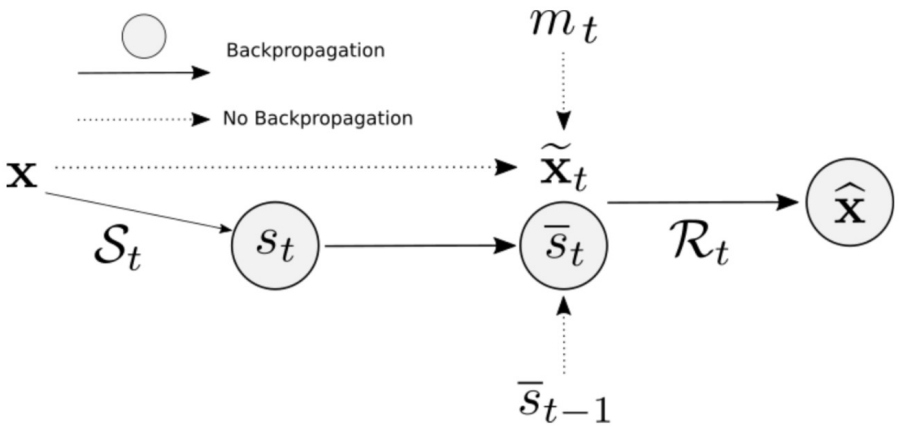

Outer loop

- Network Architecture Search (NAS)

Inner loop

- Progressive construction of the measurement subset (recursive feature elimination)
- Measurements are scored iteratively (scored at iteration t depends on score at $t-1$)

[9] Blumberg SB et al, arXiv 2022, doi: 10.48550/arXiv.2203.09268

PROSUB performance (1)

As compared to SARDU-Net, PROSUB achieves:

- *more stable and more informative sub-protocols*

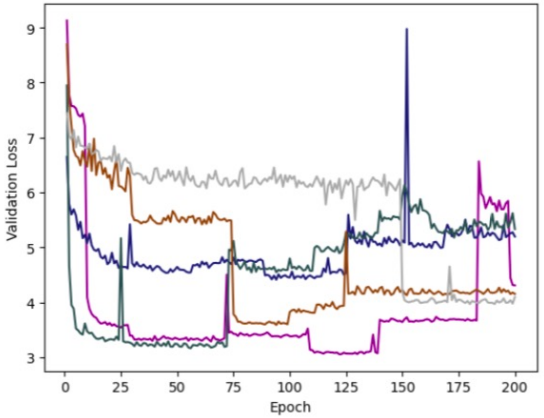

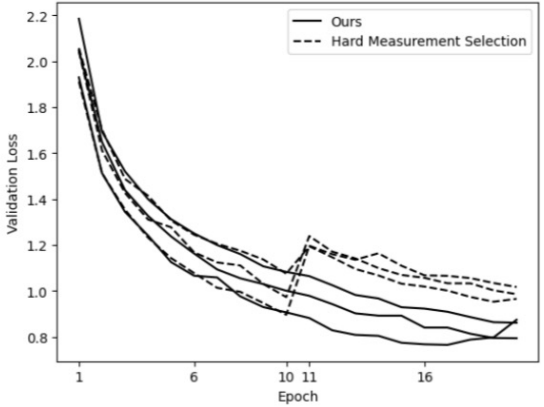

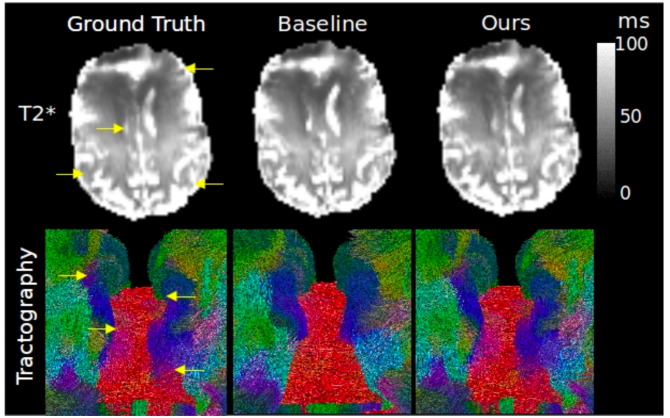

PROSUB performance (2)

As compared to SARDU-Net, PROSUB achieves:

- *more stable and more informative sub-protocols*
- *more accurate predictions of fully sampled signals*

		MUDI Challenge M for $N = 1344$			
		500	250	100	50
SARDU-Net-v1 [14,26]	Baseline	1.45 ± 0.14	1.72 ± 0.15	4.73 ± 0.57	5.15 ± 0.63
SARDU-Net-v2 [4,15]	Baseline	0.88 ± 0.10	0.89 ± 0.01	1.36 ± 0.14	1.66 ± 0.10
SARDU-Net-v2-BOF [4,15]	Baseline	0.83 ± 0.10	0.86 ± 0.10	1.30 ± 0.12	1.67 ± 0.12
SARDU-Net-v2-NAS	Baseline	0.82 ± 0.13	0.99 ± 0.12	1.34 ± 0.26	1.76 ± 0.24
PROSUB w/o NAS	Ours	0.66 ± 0.08	0.67 ± 0.09	$\mathbf{0.88} \pm 0.07$	1.54 ± 0.11
PROSUB	Ours	$\mathbf{0.49} \pm 0.07$	$\mathbf{0.61} \pm 0.11$	0.89 ± 0.11	$\mathbf{1.35} \pm 0.11$

Discussion and conclusions

- Data-driven, model-free protocol design: alternative to model-based optimisation
  - *may be useful when the model to use is not known*
  - *may be useful to shorten protocols in clinical studies if need arises*
  - *do **NOT** replace model-based optimisation*

Discussion and conclusions

- Data-driven, model-free protocol design: alternative to model-based optimisation
  - *may be useful when the model to use is not known*
  - *may be useful to shorten protocols in clinical studies if need arises*
  - *do **NOT** replace model-based optimisation*

- SARDU-Net and its extension PROSUB are tools for model-free protocol design
  - *find out which measurements are informative*
  - *potentially “enhance” a qMRI protocol*

Discussion and conclusions

- Data-driven, model-free protocol design: alternative to model-based optimisation
  - *may be useful when the model to use is not known*
  - *may be useful to shorten protocols in clinical studies if need arises*
  - *do **NOT** replace model-based optimisation*

- SARDU-Net and its extension PROSUB are tools for model-free protocol design
  - *find out which measurements are informative*
  - *potentially “enhance” a qMRI protocol*

- Future work will
  - *extend the method to convolutional architectures*
  - *test its utility beyond imaging*

Acknowledgments

Feasibility of Data-Driven, Model-Free Quantitative MRI Protocol Design: Application to Brain and Prostate Diffusion-Relaxation Imaging

frontiers in Physics

Francesco Grussu[1,2,3], Stefano B. Blumberg[2], Marco Battiston[1], Lebina S. Kakkar[4], Hongxiang Lin[2], Andrada Ianuş[5], Torben Schneider[6,7], Saurabh Singh[4], Roger Bourne[8], Shonit Punwani[4], David Atkinson[4], Claudia A. M. Gandini Wheeler-Kingshott[1,9,10], Eleftheria Panagiotaki[2], Thomy Mertzanidou[2] and Daniel C. Alexander[2]*

Progressive Subsampling for Oversampled Data - Application to Quantitative MRI

arXiv

Stefano B. Blumberg[1], Hongxiang Lin[1,3], Francesco Grussu[1,2], Yukun Zhou[1], Matteo Figini[1], and Daniel C. Alexander[1]

Acknowledgments

- **Thanks to Marco Palombo, Ting Gong, Gary Zhang for the invitation**
- Engineering and Physics Research Council (EPSRC EP/R006032/1)
- European Union Horizon 2020 programme (grant agreement 634541)
- Beatriu de Pinós Fellowship 2020 BP 00117, funded by the Secretary of Universities and Research (Government of Catalonia, Spain)
- “La Caixa” Foundation, Spain

EPSRC
Engineering and Physical Sciences Research Council

European Commission

cmic
Centre for Medical Image Computing

Generalitat de Catalunya
Departament de Recerca i Universitats

”la Caixa” Foundation

bp